Aerosol Science and Technology, 38:1123–1137, 2004
Copyright © American Association for Aerosol Research
ISSN: 0278-6826 print / 1521-7388 online
DOI: 10.1080/027868290890344

Characterization of an Ambient Coarse Particle Concentrator Used for Human Exposure Studies: Aerosol Size Distributions, Chemical Composition, and Concentration Enrichment

Ryan C. Moffet,[1] Laura G. Shields,[1] Jon Berntsen,[2] Robert B. Devlin,[3] and Kimberly A. Prather[3]

[1]*Department of Chemistry and Biochemistry, University of California, San Diego, La Jolla, California, USA*
[2]*TRC Environmental, Chapel Hill, North Carolina, USA*
[3]*National Health and Environmental Effects Research Laboratory, Office of Research and Development, United States Environmental Protection Agency, Research Triangle Park, North Carolina, USA*

The goals of the experiments described herein involve determining in real time the size, concentration enrichment, and chemical composition of coarse-mode (>2.5 μm) and fine-mode (<2.5 μm) particles within the nonconcentrated and concentrated flows of a coarse particle concentrator used for human exposure studies. The coarse particle concentrator was intended to concentrate ambient particles in the $PM_{10-2.5}$ size range before sending them into a human exposure chamber. The aerodynamic size and chemical composition of particles in the upstream and downstream flows of the concentrator were monitored with an aerosol time-of-flight mass spectrometer (ATOFMS) for fixed time intervals over the course of three days. Based on the ATOFMS results, it was found that there was no change in the composition of the ten major particle types observed in the upstream and downstream flows of the concentrator under normal operating conditions. Furthermore, no new particle types were detected downstream that were not detected upstream of the concentrator. A characterization of the aerosol chemical composition and its dependence on sampling conditions is also discussed. Aerosol size distributions were measured with three aerodynamic particle-sizing (APS) instruments sampling simultaneously from different regions of the concentrator. The APS size distributions were used to scale ATOFMS data and measure the ambient concentration factors for the coarse particle concentrator and the exposure chamber. The average concentration factor (ratio of inlet number concentration to the outlet number concentration) for the particle concentrator was 60 ± 17 for the 2.5–7.2 μm size range before dilution and transport to the exposure chamber. It was observed that not only were coarse particles being concentrated but fine (<2.5 μm) particles were being concentrated as well, with concentration factors ranging from 2–46 for aerodynamic particle sizes from 0.54–2.5 μm.

Received 11 February 2004; accepted 16 September 2004.

All members of the Prather research group at UCSD were extremely helpful during every stage of this study. David Kosnikowski for TRC Environmental gave assistance in operating the coarse concentrator used in this study. The research presented is supported by the University of Rochester EPA PM Center under grant R827354. This report has been reviewed by the National Health and Environmental Effects Research Laboratory, United States Environmental Protection Agency, and approved for publication. Approval does not signify that the contents necessarily reflect the views and policies of the Agency nor does mention of trade names or commercial products constitute endorsement or recommendation for use.

Address correspondence to Kimberly A. Prather, Department of Chemistry and Biochemistry, University of California, San Diego, La Jolla, CA 92093-0314, USA. E-mail: kprather@ucsd.edu

INTRODUCTION

A large number of epidemiology studies indicate that particulate matter (PM) less than 10 μm in diameter (PM_{10}) is associated with adverse health effects including mortality (Dockery and Pope 1994; Dockery et al. 1992, 1993; Gamble 1998; Peters et al. 1997). However, mortality is not the only effect of concern—other indicators, such as increased emergency room visits due to asthma and respiratory problems, have also been observed (Gavett and Koren 2001; Leikauf 2002). Recent toxicology studies have shown that coarse PM may stimulate the release of inflammatory mediators in the lung and thus may be linked with respiratory problems (Monn and Becker 1999). Determining whether coarse-mode particles cause adverse health effects, and if so to what extent, is extremely important for the health effects community and policy makers.

In order to characterize further the health effects of coarse particles, a system was developed to expose humans to concentrated ambient aerosols. This exposure system was built using a coarse particle concentrator implementing virtual impaction (Demokritou et al. 2003) and an exposure chamber. The coarse

particle concentrator was designed to concentrate particulate matter in the $PM_{2.5-10}$ range, while at the same time providing a large enough flow of concentrated aerosol to fulfill human breathing requirements. The coarse concentrator has a low pressure drop between impaction stages to reduce the loss of semivolatile compounds that may be on the PM. For this reason, the change in chemical composition between the upstream aerosol flow and the concentrated downstream aerosol flow should be minimized. However, since the vapor-phase semivolatile species are not concentrated along with the PM, the equilibrium may be disturbed, leading to a possible chemical change in the aerosol. In this manuscript, we describe an experiment in which particles in the upstream and downstream flows were analyzed with aerosol time-of-flight mass spectrometry (ATOFMS) to determine if there are any chemical differences induced by the concentration process.

We also took the opportunity to monitor the chemical composition of particles during human exposure studies to determine the chemical variability of coarse particles over short time periods. Determining the size-segregated chemical composition of an aerosol is an essential part of any human exposure study in order to correlate particle types with any deleterious health effects that may occur. An advantage of using a real-time, single-particle instrument such as the ATOFMS in exposure studies is the ability to measure chemical changes with short temporal resolution. This information can be used to establish correlations between particle composition and other real-time measurements taken during human exposure studies such as human heart rate variability. Traditionally chemical analysis is accomplished by collecting a predetermined particle size range on a variety of filter media. However, when particulate matter is collected in such a manner, there is potential for loss of semivolatile compounds (compounds that partition appreciably to both the particle and gas phases under normal ambient conditions) that may contribute significantly to the toxicological properties of the aerosol (Eatough et al. 2003; Seagrave et al. 2003). Since the particles are under vacuum for less than 1 ms in the ATOFMS, loss of semivolatile compounds is minimal, making the analysis of these species more feasible (Tobias 2000). Further problems are associated with bulk measurements because chemical reactions may occur on the filter substrate between sample collection and analysis, which may change the toxicological properties of the particulate matter. It can also be difficult to collect enough particulate matter for mass measurements during a typical human exposure studies (which only last for 2 h). ATOFMS can provide a relative measure of the amount of species on certain particle types, but the use of laser desorption/ionization can introduce detection biases and challenges for chemical quantitation. Additionally, the size distribution obtained from the ATOFMS is not representative of the actual aerosol size distribution due to the decreasing detection efficiencies of smaller sizes. The latter point is overcome in this study by using a method that involves scaling the ATOFMS measurement to another real-time size distribution measurement acquired with an aerodynamic particle sizer.

This article reports results from a study performed to monitor the size and chemical composition of aerosol particles in real time during human exposure studies carried out at the EPA Human Studies Facility in Chapel Hill, NC. During three characterization studies, the chemical compositions of the inlet and outlet of the concentrator were monitored to measure any changes induced by the concentrator. Additionally, using several APS instruments, concentration factors at the outlet of the concentrator are presented to provide information on the levels of coarse and fine particles to which the human subjects are exposed.

EXPERIMENTAL METHODS

The experimental setup used in this study is shown in Figure 1. Ambient air was drawn in at 5000 lpm from the rooftop of the EPA Human Studies Facility in Chapel Hill, NC and transferred downward into the building ($T = 21°C$) to the PM_{10} inlet of the concentrator via a 16 ft long duct with a 1 ft outer diameter. The size-selective inlet and the virtual impactors are the same as those used in Demokritou et al. (2003). The major outward flow was 4500 lpm for the first impaction stage, while the major outward flow out was 450 lpm for the second impaction stage, giving a 50 lpm concentrated aerosol flow. The concentrated aerosol flow had a theoretical concentration factor (CF) of 100 (obtained from the ratio of the inlet flow to the outlet flow), assuming coarse particles have 100% transmission. After flowing out of the virtual impaction stages, the concentrated aerosol was diluted with a sheath of conditioning air (150 lpm, RH ~5%), which was introduced around the concentrated aerosol flow. This conditioning air was added to provide enough airflow for the human subjects' breathing requirements and to condition the air to moderate the outside temperature and relative humidity changes. The flow velocities of the conditioning air and the concentrated air were matched to ensure laminar flow. After the 150 lpm conditioning air was added, the overall theoretical concentration factor of the aerosol was 25.

Particle size distributions were measured with two model 3321 aerodynamic particle sizer (APS) instruments and one model 3310 APS instrument (TSI Inc., St Paul, MN, USA). The APS instrument measures aerodynamic particle size by measuring the particle time of flight between two laser beams and relating this time to aerodynamic diameter. The APS 3321 instruments were redesigned to eliminate coincidence errors and errors associated with the recirculation of particles inside the scattering region of the instrument. As shown in Figure 1, the two 3321 APS instruments were located between the PM_{10} inlet and the first virtual impaction stage, while the second 3321 APS instrument was located between the second virtual impaction stage and the dilution air. The 3310 APS instrument was located between the Data RAM (Thermo) and versatile air pollutant sampler (VAPS; University Research Glass). The VAPS was used to collect samples on filters to compare both mass and chemical composition. The APS 3310 measured the aerosol concentration

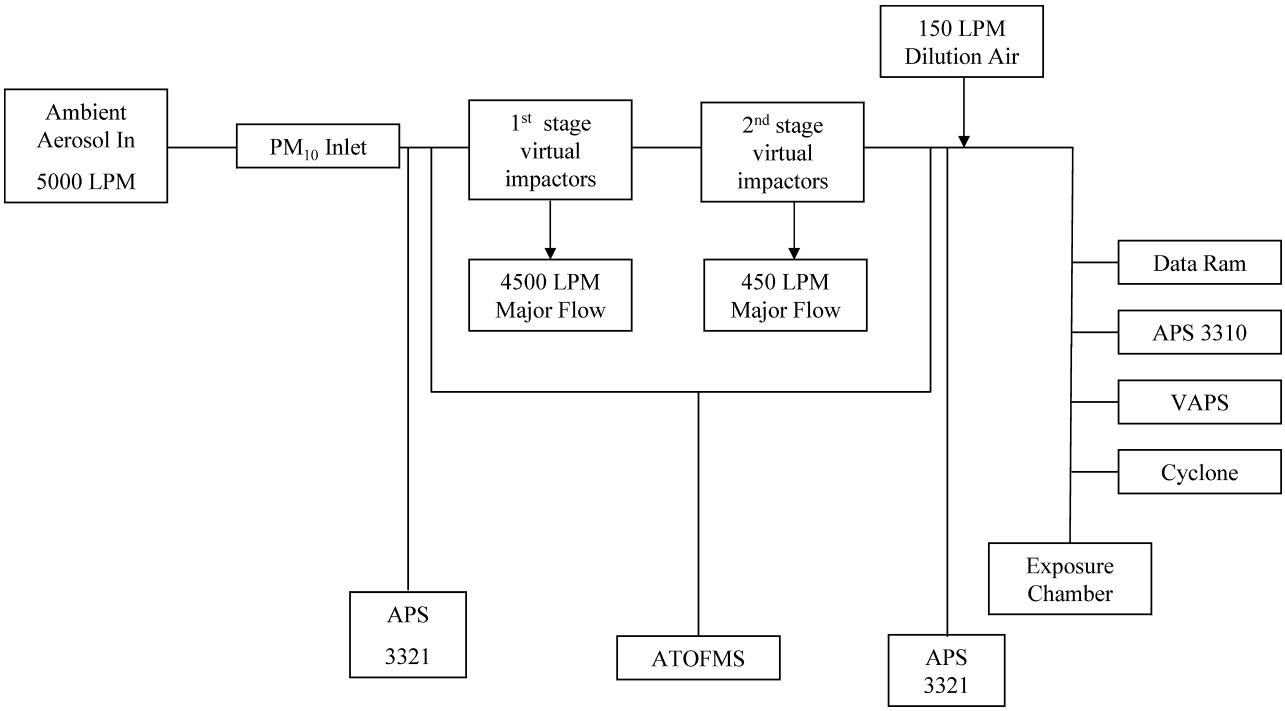

Figure 1. Experimental layout for the coarse concentrator/exposure chamber studies.

just after mixing with the dilution air and before the exposure chamber. The 3321 APS instruments were factory calibrated prior to this experiment to ensure both the particle size and number concentration were accurate and consistent. All sampling lines to the APS and ATOFMS were fabricated with 1/2″ and 3/8″ stainless steel tubing, respectively. All sampling probes were aligned parallel to the direction of flow, having diameters and flow rates such that anisokinetic losses were negligible.

The concentrations given by two APS 3321 instruments typically differed by 2–22% in the individual size bins on the same aerosol sample. Since the two instruments were running simultaneously in different positions to calculate concentration factors in various regions of the concentrator/exposure chamber system, their readings needed to be made comparable with one another. To accomplish this, scaling factors between the two instruments were experimentally determined for each APS size bin as follows. Let the scaling factor be defined as

$$\gamma_i = N_{av}/N_i, \quad [1]$$

where N_{av} is the average number concentration reading between the two APS instruments on the same aerosol sample, and N_i is the raw number concentration given by the ith APS on that same sample. The value of γ_i was determined during a separate 25 min study in which the two APS instruments sampled the same aerosol flow through identical sampling lines. A scaled number concentration that is consistent between the two instruments is then given by Equation (2):

$$N_{sc} = \gamma_i N_{s,i}, \quad [2]$$

where $N_{s,i}$ is the raw experimental number concentration to be scaled (for a different aerosol sample than N_i). All APS number concentrations ($N_{s,i}$) collected during the characterization and exposure studies were adjusted according to Equation (2). Since the scaling factors changed between the concentrated and non-concentrated aerosol streams, different scaling factors for the different streams were determined.

A transportable ATOFMS instrument (Gard et al. 1997) was used for the characterization of particle size and chemical composition in this study. In Figure 1, the ATOFMS sampled particles from the coarse concentrator system (1) directly after the PM_{10} size-selective inlet (before passing through the virtual impactors), or (2) after the second stage of impaction but before the dilution air, was supplied to the system. The sampling lines for the APS systems and the ATOFMS were similar in their materials (stainless steel), probes, bends, and lengths as to enable reliable scaling of the ATOFMS data to the APS data. A scaling function (S_{ATOFMS}) was used to scale the ATOFMS number concentration for different particle classes to an APS number concentration. S_{ATOFMS} was determined as a function of aerodynamic diameter (using the 37 logarithmically spaced APS bins between 0.561 and 7.498 μm) according to the relation

$$S_{ATOFMS} = N_{aps}/N_{ATOFMS}, \quad [3]$$

where N_{aps} is the APS number concentration and N_{ATOFMS} is the ATOFMS number concentration on the same sample. Scaling in this manner is a semiquantitative way to correct for the size bias and low transmission efficiency of the ATOFMS inlet

(Allen et al. 2000). APS and ATOFMS data for the entirety of each exposure or characterization study were used to calculate S_{ATOFMS}.

Two different types of experiments were performed during sampling periods consisting of exposure experiments and characterization experiments. Exposures refer to sampling periods when a human subject was in the exposure chamber. The two exposure experiments that were monitored with the ATOFMS took place on 8/25/03 from 9:57–11:57 and on 8/27/03 from 9:27–11:27, EDT. The characterization of the concentrator refers to studies in which the inlet and outlet of the concentrator were monitored for 1 or $^1/_2$ h time periods alternating the ATOFMS measurements between the upstream and downstream flows of the concentrator. The characterization sampling periods occurring from 12:00–21:00 EDT on 8/26/03, 12:00–20:00 EDT on 8/27/03, and 13:02 EDT on 8/28/03 were used to determine whether or not the virtual impactors chemically altered the particles.

ATOFMS data from the characterization experiment and the exposure studies were analyzed with ART-2a (Song et al. 1999), using a vigilance factor of 0.7, a learning rate of 0.05, and 20 iterations. ART-2a is an artificial intelligence algorithm that sorts single-particle mass spectra into specific particle types or clusters. Using a vigilance factor of 0.7 with ART-2a analysis, 52,134 particles were analyzed to produce 105 clusters with 5 or more particle members. The top 10 clusters accounted for 87% of all particles. Due to inhomogeneities in the laser desorption/ionization laser beam, there was variability in the relative abundances of some of the major peaks that were instrumental instead of chemically related (Wenzel and Prather 2004). Taking this into account, the clusters were manually regrouped into 10 general classes that explained 98% of the particles. The 10 types were labeled according to the dominant species present (elemental carbon (EC)—with no negative spectrum (EC-no neg), Long EC (having EC peaks above m/z = 100), Calcium dust (Ca Dust), Potassium (K)-sulfate—organic carbon (OC) (K-sulfate-OC), EC-K-sulfate, Dust, K-Phosphate, Sea Salt, OC) while the rest were placed in a "No ID" class. Ten classes were settled upon for two reasons: (1) to keep the statistics high enough to enable reliable comparisons, and (2) the other minor particle classes represented a very small fraction (<2%) of the particles. Criteria used to distinguish the classes are discussed in the results and discussion section.

For comparing the chemical compositions in the exposure and characterization studies, raw number concentrations (N_r) of the particle classes were scaled to give a scaled number concentration (N_s) according to the relationship

$$N_s = S_{ATOFMS} N_r, \quad [4]$$

where S_{ATOFMS} was introduced in Equation (3). Again, it should be noted that because the unscaled ATOFMS number concentrations are not the "true" atmospheric particle concentrations, this scaling procedure is used to transform the ATOFMS number concentration into a scaled APS number concentration for different particle classes. Scaling to the APS compensates for the strong dependence the transmission efficiency of the ATOFMS inlet has on particle size.

Sampling Conditions

Two important factors when sampling from the coarse concentrator are the temperature and relative humidity (RH) of the ambient air being introduced. When a relatively warm and humid aerosol containing ambient air sample is transferred into the concentrator at room temperature, there is a possibility for condensation to occur. The temperature around which this process occurs and the air parcel becomes saturated is called the *dew point temperature* (T_d). The Clausius Clayperon relationship can be used to calculate the dew point temperature. The results of this calculation over the entire study are shown in Figure 2, which shows T_D, outside temperature, and the chamber inlet temperature during the characterization and exposure studies. The chamber inlet temperature is the temperature of the aerosol flow going into the chamber. This temperature was close to that of the building. During the first exposure and characterization studies, the dew point temperature was lower than the inlet temperature of the exposure chamber. During the second exposure and the second and third characterization studies, the dew point was above chamber inlet temperature.

RESULTS AND DISCUSSION

Concentration Factors and APS Size Distributions

There was strong evidence for condensation events during the second exposure study and the last two characterization studies. Initial evidence of condensation was indicated by the accumulation of liquid water in the PM_{10} inlet. In addition, the aerosol size distributions in Figure 3 show a size shift for the distributions measured at the inlet and outlet during two different studies. Figure 3a shows the APS size distributions for the first characterization study where the room temperature was above the dew point temperature, and Figure 3b shows the distributions for the second characterization study when room temperature was below the dew point temperature. All times where the dew point temperature went above room temperature and the size distributions widened will be referred to as *condensation events*. Even when the outlet number concentration during the condensation events was divided by the concentration factor, there was still a difference between the inlet and outlet distributions, suggesting additional condensation occurring as the particles were being sampled into the building.

For some highly hygroscopic particles, condensation occurs at temperatures below T_D, while for hydrophilic particles condensation occurs above T_D. Thus, particles having different compositions may have different growth characteristics under saturated conditions. To determine whether there was any chemical bias for water condensation, we examined the size distribution shifts for several particle classes and found consistent changes for all particle types.

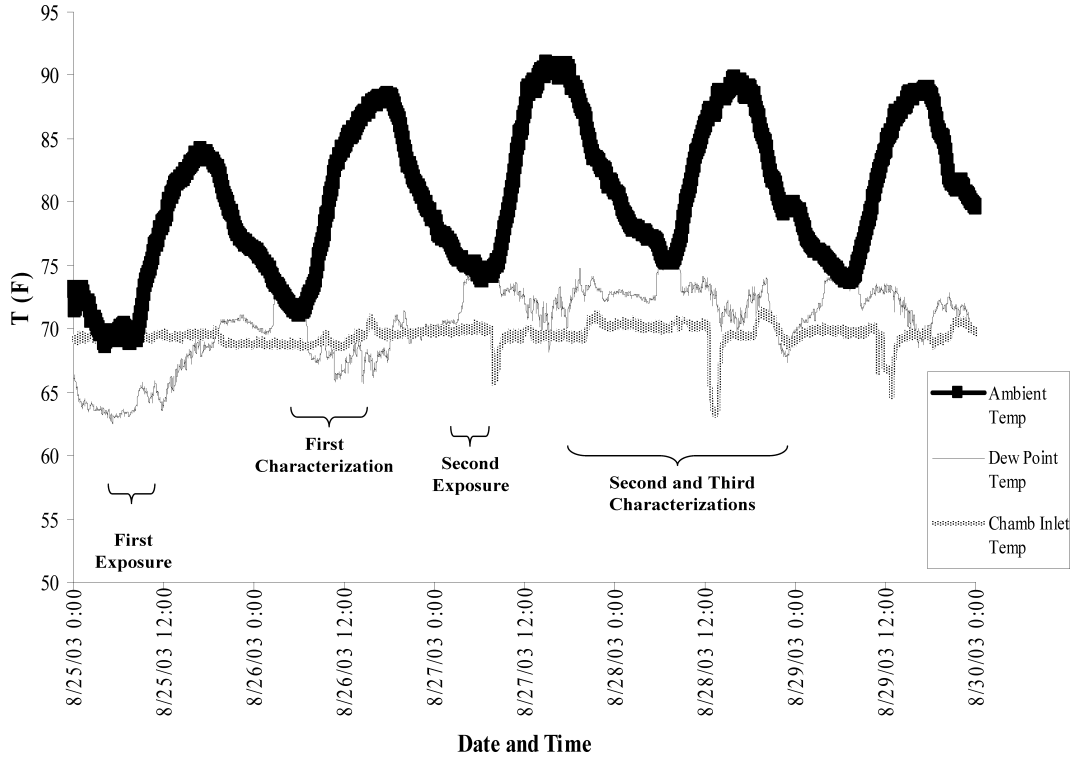

Figure 2. Temperature conditions during the time of the coarse concentrator studies.

From the size distributions measured in the various regions, the concentration factors were calculated and the results are shown in Table 1. The concentration factor (CF) was calculated by dividing the inlet number concentration by the outlet number concentration for each size bin. The undiluted concentration factor agrees well with the results obtained from the work of Demokritou et al. (2003). In that work, Demokritou et al. determined a concentration factor of 68 using hollow glass spheres having a mean diameter of 3.68 μm. In this study, the concentration factors were determined using ambient aerosols having a mean diameter of 0.71 μm that gave an average concentration factor of 60 $\pm$ 17 for coarse-mode particles (2.5–7.2 μm) before dilution. The concentration factors in Table 1 are seen to fluctuate dramatically at higher sizes due to more uncertainty in counting statistics. There are two possible reasons for the poor counting statistics at the higher sizes: (1) very low particle concentrations at these sizes, and (2) low the APS transmission efficiency at these higher sizes.

One topic that has not been addressed in previous studies (Demokritou et al. 2003) that may be of interest to the health effects community is the concentration factor for fine particles. The cutpoint of an inertial impactor is defined as the size where 50% of the particles of a given size follow the major flow and 50% follow the minor flow (Hinds 1999). Therefore, if the ratio of flows is greater than a factor of 2, particles below the cutpoint will still be concentrated. This is clearly demonstrated in the present study since concentration factors ranging from 2 to 46

Table 1
Concentration factors (CF) before and after dilution

D_a (μm)	CF before dilution	CF after dilution	D_a (μm)	CF before dilution	CF after dilution
0.54	2	0	2.13	23	17
0.58	2	0	2.29	31	14
0.63	2	1	2.46	46	18
0.67	2	1	2.64	59	17
0.72	2	1	2.84	68	17
0.78	2	1	3.05	64	17
0.84	2	2	3.28	63	17
0.90	2	1	3.52	61	13
0.97	2	1	3.79	64	15
1.04	3	1	4.07	63	13
1.11	3	1	4.37	58	14
1.20	4	2	4.70	72	15
1.29	4	3	5.05	83	18
1.38	5	3	5.43	71	9
1.49	5	3	5.83	63	8
1.60	6	6	6.26	38	6
1.71	8	8	6.73	71	4
1.84	10	11	7.23	11	4
1.98	15	13			

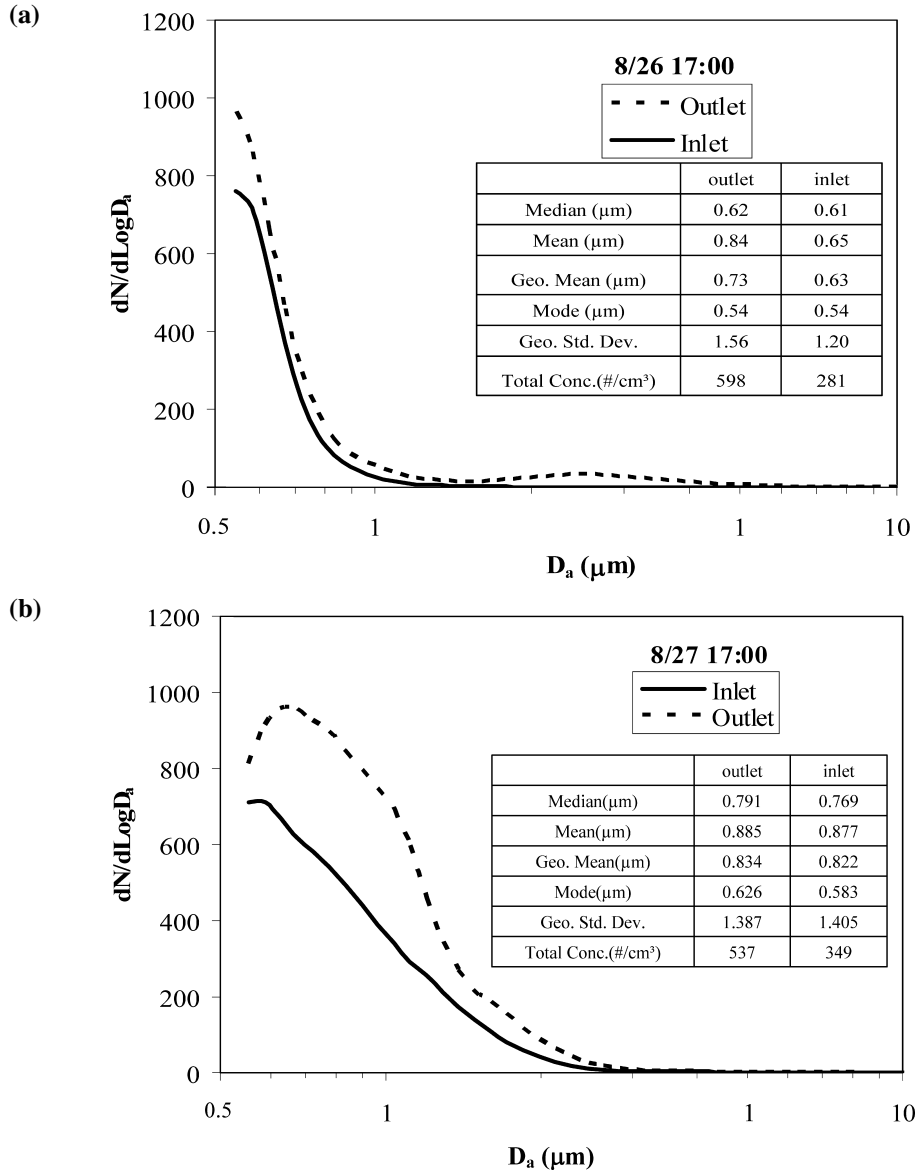

Figure 3. (a) Size distributions at the inlet and outlet of the concentrator during normal sampling conditions. (b) Size distributions at the inlet and outlet during a condensation event.

were obtained for particles with D_a between 0.54–2.46 μm. This is an important finding as particles in this size range can have significantly different compositions and sources than coarse-mode particles (Hughes et al. 2000). Since the cutpoint region is characterized by a fairly sharp cutoff, the concentration factors vary strongly with D_a. The concentration factors after addition of dilution air differed from the undiluted concentration factors by a factor of 4–5 for coarse-mode particles, which is consistent with the dilution ratio of the concentrated to diluted streams.

The above concentration factor analysis allows direct comparison with Demokritou et al., but it is also important to estimate the relative contribution both the coarse and fine modes have to particle mass before and after undergoing the concentration process. To estimate the relative contributions to coarse- and fine-mode mass, we assumed a density of 1 g/cm^3 and calculated the coarse- and fine-mode mass fractions using the APS data. Although this is a simplistic assumption that neglects the true densities and shape factors, it is sufficient for the comparisons that follow. It was found that before concentration, 77% of the particles contributed to the fine-mode mass and 23% of the particles contributed to the coarse-mode mass. In the chamber, the trend reversed so that 25% of the particles contributed to the fine-mode mass and 75% of the particles contributed to the coarse-mode mass. These numbers are consistent with the mass fractions derived from the cyclone for the concentrator outlet just before the chamber; with these measurements showing that 31%

of the mass was in the fine mode and 69% of the mass was in the coarse-mode. Filter data also show that the concentration during the exposures is fairly high, being 56.12 and 102.83 $\mu g/m^3$ during the first (8/25) and second (8/27) exposures, respectively.

When interpreting the results in this section with regards to health effects, it is crucial to keep in mind how the size distributions of the particles change when number, surface area, and mass are used. It may be important that the particles in the fine mode are being concentrated when considering the health effects linked with the total surface area and number concentration of the particles. However, if one is mainly concerned with the effects of particle mass on health, then the concentration of particles at or below the cutpoint of the concentrator becomes less of an issue.

Raw ATOFMS Size Distributions and Scaling Function (S_{ATOFMS})

Under normal ambient conditions, particles are not frequently detected over 3 μm with the ATOFMS. Figure 4 shows a size distribution produced using raw ATOFMS counts for concentrated and nonconcentrated aerosol streams. These raw ATOFMS counts include only particles that were chemically analyzed by the ATOFMS. When sampling the concentrated stream of the coarse particle concentrator, particles above 4 μm were commonly detected with the ATOFMS, an observation that supports their enrichment. Figure 4 also shows a peak occurring at $\sim$1.7 μm, corresponding to the most efficiently focused size into the ATOFMS.

As mentioned in the experimental section, S_{ATOFMS} is the factor by which we need to multiply the ATOFMS number concentration to obtain a number concentration that has been standardized to the APS instruments. S_{ATOFMS} was calculated every hour for the duration of the characterization and exposure studies. Figure 5a shows the hourly scaling functions calculated for the first characterization study. As shown in the figure, the scaling function remained relatively constant throughout the period of one day. Figure 5a also shows that the scaling function is relatively constant between concentrated and nonconcentrated aerosol streams. However, at the extremes of the scaling function (i.e., for very large and very small D_a), the function shows larger oscillations due to the smaller sample sizes used for averaging.

Figure 5b shows S_{ATOFMS} as a function of aerodynamic diameter for the three characterization and two exposure experiments. The scaling functions can be used for the determination of any detection efficiency changes for a given aerosol concentration or composition. The S_{ATOFMS} did not change much throughout the period of one day; however, it changed significantly on a day-to-day basis, most likely due to changes in ambient temperature and relative humidity (RH). During the first exposure and characterization experiments, the RH was low, and there was

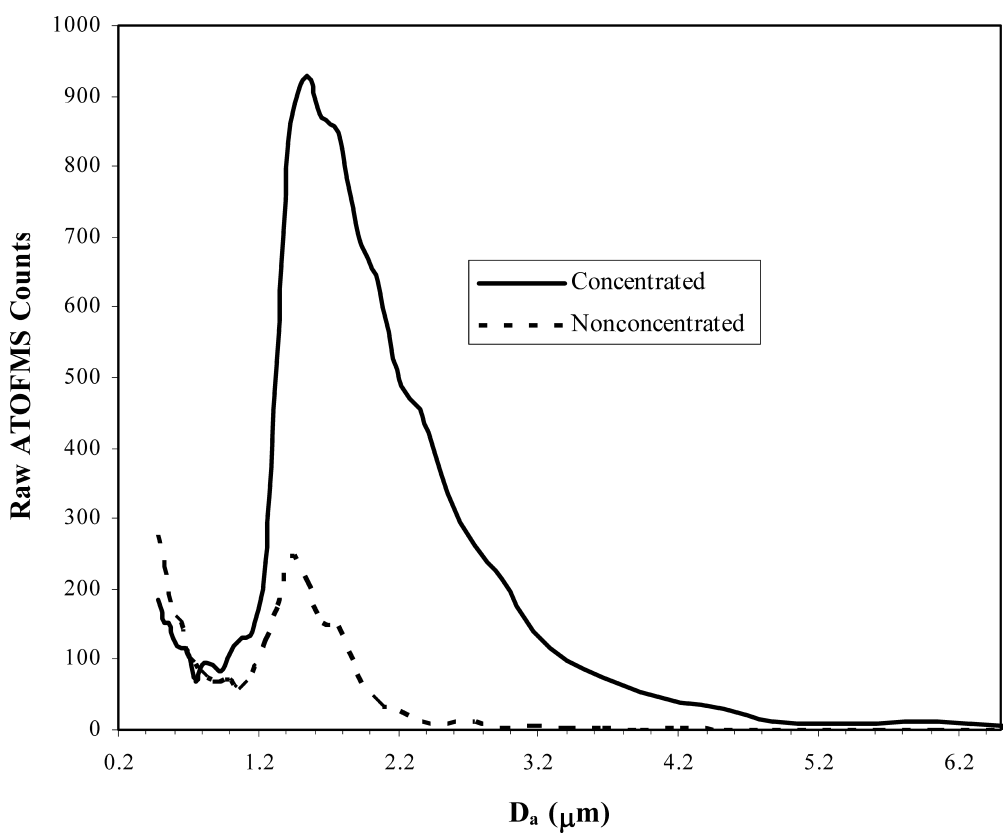

Figure 4. Unscaled size distributions produced by ATOFMS with the coarse concentrator on and off.

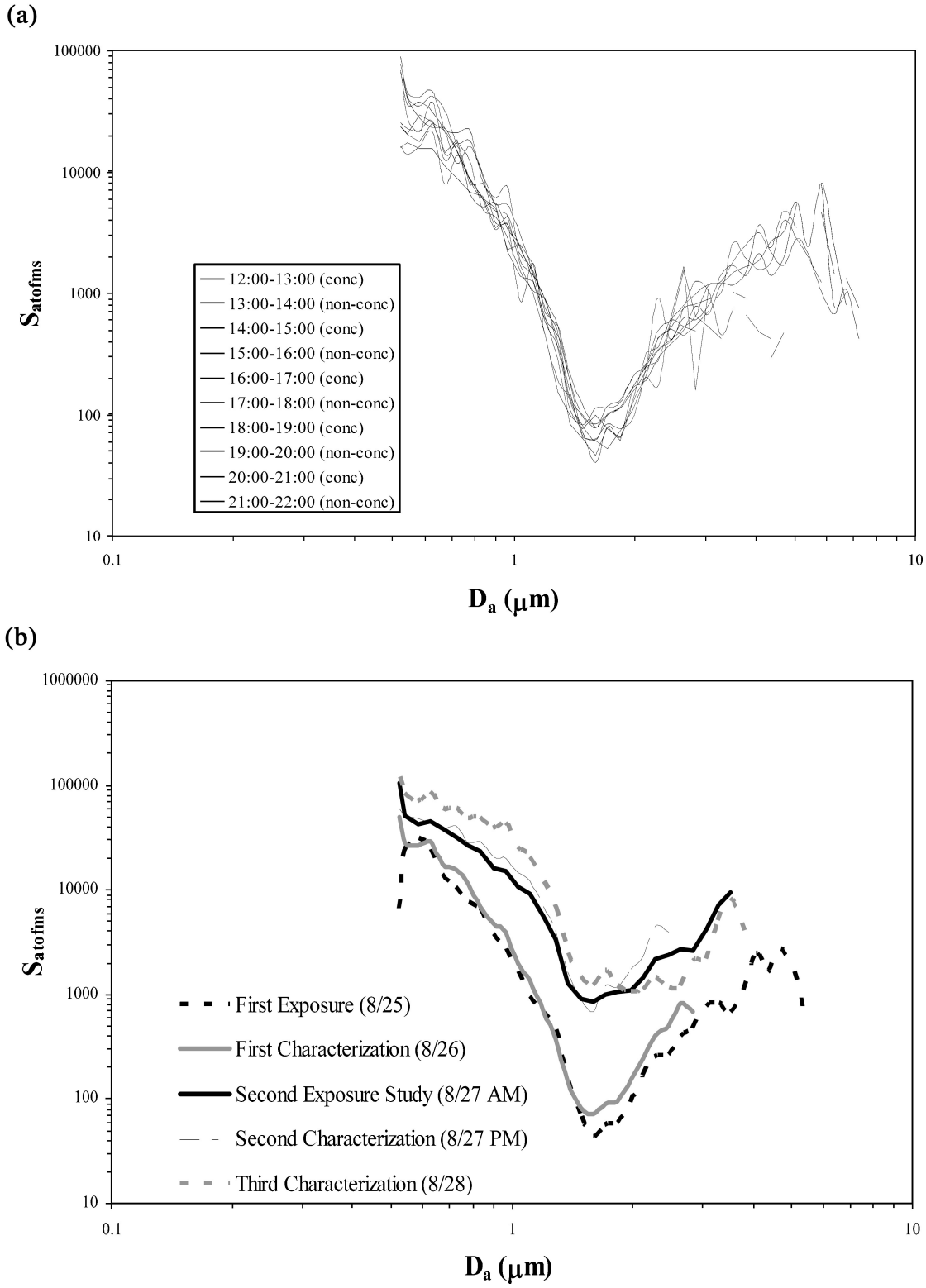

Figure 5. (a) Hourly scaling functions for the first characterization study. (b) Scaling functions derived for important time frames during the coarse concentrator studies. The curves represent averages of one hour samples for the entirety of each study.

no condensation occurring on the particle surfaces. All of the other experiments were accompanied by high RH, causing condensation of water on particle surfaces. Condensation events are evident in the ATOFMS data by a decrease in the detection efficiency, as illustrated by the overall increase in S_{ATOFMS} for the periods when condensation was occurring. This is most likely due to the fact that inorganic aqueous aerosols typically have higher ionization thresholds and produce lower ion currents (Neubauer et al. 1997), yielding a smaller fraction of mass spectra thereby raising S_{ATOFMS}.

ATOFMS Chemical Analysis

As described in the Experimental Methods section, the ambient particles detected in North Carolina could be divided into 10 major chemical types based on the distinct patterns in their mass spectra and ART-2a analysis. The most prevalent class observed for coarse-mode particles was the K-Phosphate class. This class was dominated by negative ion phosphorous (PO_3 and H_2PO_4 at m/z = −79 and −97) and positive ion K (m/z = +39) peaks. Possible contributors to the K-Phosphate class include coal combustion, vegetative detritus, biomass burning, pollen, and road dust (Guazzotti et al. 2003; Liu et al. 2003; Noble and Prather 1997). Further ATOFMS source tests will allow us to determine which of these sources is most likely upon comparison of particle signatures.

Figure 6 shows a soil/dust particle that was labeled as the dust class due to its intense aluminosilicate peaks. Silicates and aluminum are the major markers for crustal material (Guazzotti et al. 2001; Silva et al. 2000). Silicate ions were observed in the negative spectrum. In the same particle, aluminum appeared in the positive ion spectrum in the atomic ion form, with the oxides of aluminum in the negative spectrum. This particular soil particle contains markers consistent with the fact that the North Carolina Piedmont soils are composed mainly of kaolinite ($Al_2Si_2O_5$-$(OH)_4$), which is an aluminosilicate mineral (Rice et al. 1985; Robarge 2003, personal communication).

An interesting subclass of the K-Phosphate class was the amine particle type shown in Figure 7. The amine class was labeled as such based on the presence of major ion peaks at m/z = 58, 59, 60, 74, 86, and 104, and minor unknown peaks at m/z = 154 and 184. With the exception of the peak at m/z = 104, the other major peaks are all consistent with those detected in previous field studies in Atlanta and in laboratory studies with pure alkyl amines (Angelino et al. 2001). However, the amines in this study appear to be a different organic species and from a different source due to the fact that they are present only in the coarse mode and are coupled with a large potassium ion signal. Furthermore, these peaks did not show any correlation with RH or an anticorrelation with temperature, suggesting that this class is not semivolatile and therefore does not undergo a significant amount of gas-to-particle partitioning. The identity of the peak m/z = 104 is unknown, but may represent the protonated molecular ion (i.e., MH^+) of a nitrogen-containing organic species. The isotopic ratio for 104/106 does not support the identification of the peak at m/z = 104 as K_2CN—a peak observed in previous studies by our group (Silva and Prather 2000). Possible sources for the amines and nitrogen-containing organic species include (1) swine and/or poultry farms, (2) combustion activities, (3) synthetic or natural fertilizers, (4) sea spray, and (5) reactions of NO_x with biogenic compounds (Cornell et al. 2003). It should be noted that North Carolina is known to have high concentrations of ammonia and other nitrogen-containing organic compounds due to large swine and poultry operations (Robarge et al. 2002; Walker et al. 2000).

Although the focus of the coarse concentrator experiments was on the $PM_{2.5-10}$ fraction, the $PM_{2.5}$ fraction still made up the largest portion of the particles sampled (by number) in this study as discussed above (Figures 3 and 4). The two classes making up the bulk of the $PM_{2.5}$ fraction were the classes containing EC and OC. The mass spectrum of a typical particle that was classified as "long EC" is shown in Figure 8. This class was dominated by carbon clusters appearing in 12 m/z unit increments extending

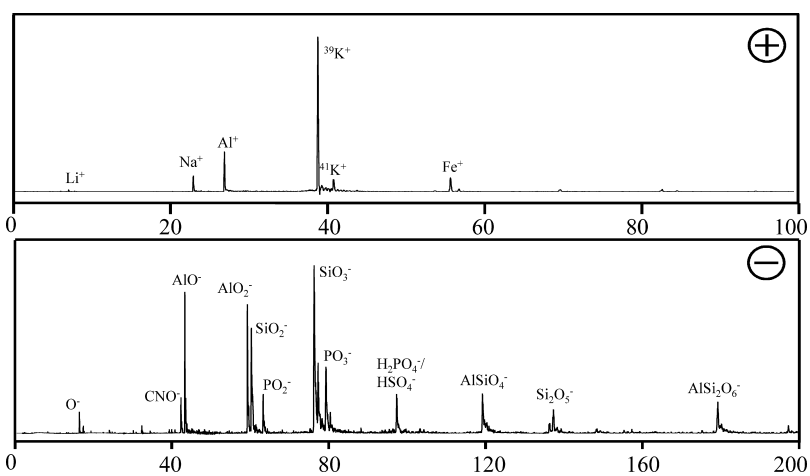

Figure 6. A single particle member of the dust class.

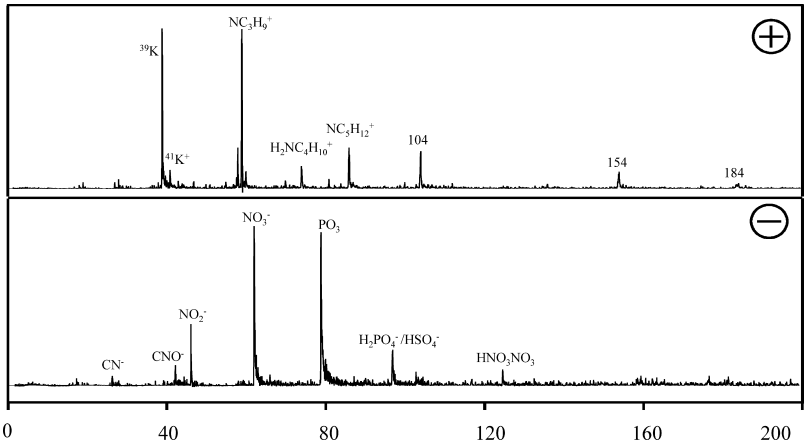

Figure 7. A single particle member of the amine subclass. This class was common only in coarse-mode particles and always occurred with a large ^{39}K signal.

out to masses beyond m/z = 100. The other EC classes were typified by carbon peaks at lower m/z units such as 12 and 36, and they either produced no negative spectrum or had sulfates and EC peaks in the associated negative spectrum. The lack of negative ion peaks was most likely an instrumental issue. A typical OC spectrum is shown in Figure 9. The spectra for particles in this class contain the usual organic peaks at m/z = +12 and +27, but additionally they have major peaks at m/z = +43 and +55 corresponding to either oxidized carbon compounds ($^{43}C_2H_3O^+$ and $^{55}C_3H_3O^+$) or nitrogen-containing organics ($^{43}CHNO^+$ and $^{55}C_2HNO^+$). The OC class also shows a dominant peak at m/z = +18, most likely due to secondary $^{18}NH_4^+$ but also possibly due to the presence of other nitrogen-containing organic species.

Several different types of secondary species were found on all particles in the PM_{10} size range. From Figures 6, 7, and 8, bisulfate $[^{97}HSO_4]^-$ and nitrate $[^{62}NO_3]^-$ were detected on a variety of particle types. Other possibilities for secondary species include oxidized OC and ammonium. Throughout the study, ammonium (m/z = 18) and oxidized OC (m/z = +43 and +55) showed a strong positive correlation with RH over all size ranges. At night the fraction of particles detected having ammonium and OC was as high as 65%. During the daytime, when the exposure studies were carried out, the percentage of detected particles having ammonium and oxidized OC was near the daily minimum of 30–40%. These observations are consistent with previous observations made by our group in the southeastern United States (Liu et al. 2003). Depending on the availability of HNO_3 or H_2SO_4 in the atmosphere, ammonia may react with these species in the gas phase to produce secondary NH_4NO_3 or NH_4HSO_4 on ambient particles (Finlayson-Pitts and Pitts 2000). These observations suggest there was a significant amount of gas-to-particle partitioning occurring in this area. The presence of ammonium, sulfate, and nitrate is important from a health effects perspective due to their reactions with strong acids, which are known

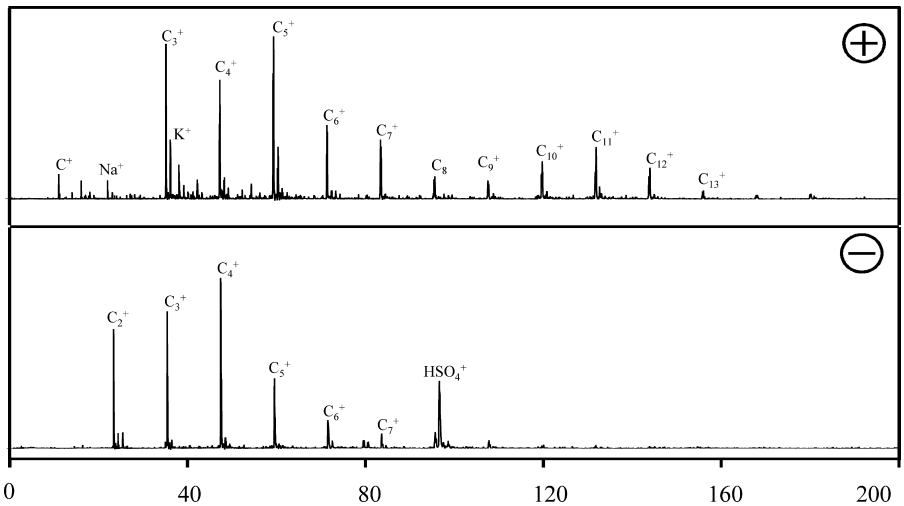

Figure 8. A single particle member of the long-EC class.

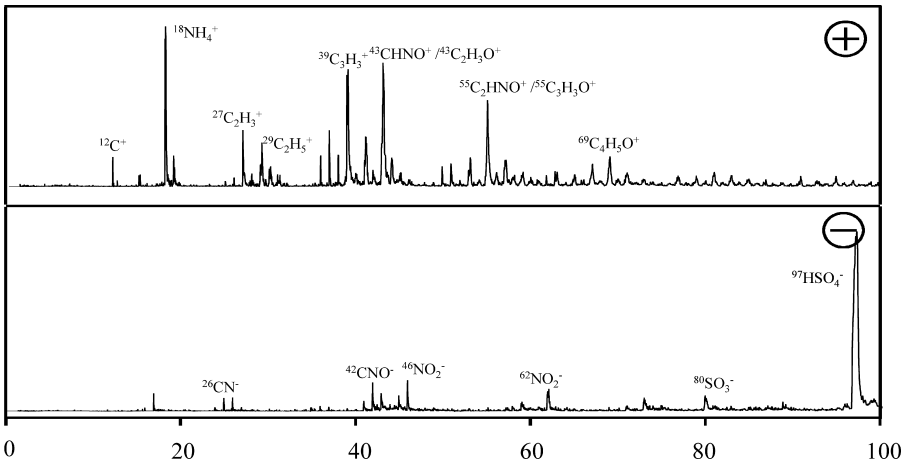

Figure 9. A single particle member of the OC class.

to be associated with the inflammation of the throat and lungs (Lippmann 1989).

Chemical Characterization of the Concentrator and Exposure Studies

For the purpose of characterizing the coarse particle concentrator, a sampling protocol was developed where the nonconcentrated flow of the concentrator was measured for a set time interval followed by a measurement of the concentrated flow for the same duration of time. For the first and second characterizations this time interval was 1 h and for the third characterization study this time interval was 30 min. Particles from all time intervals were classified with ART-2a into the ten major particle types discussed above. Results from the characterization studies are shown in Table 2.

Table 2 shows that the coarse concentrator does not significantly affect the particle composition. The first row in Table 2 shows the uncertainty associated with each particular column. The uncertainty is given by Poisson statistics, where the variance associated with the measurement is equal to the square root of the number of particles used to calculate the ATOFMS number concentration. The uncertainty is seen to be large where the particle counts are low—particularly above 2.5 μm. Although the measurements for the coarse-mode particles are associated with a much higher uncertainty, measurements for fine-mode particles also indicate that the concentrator does not change the chemical composition of the particles with a higher degree of confidence.

To determine if the concentrator affected the partitioning of the semivolatile species onto the particles, two analysis steps

Table 2
Percent of particle types for the upstream (US) and downstream (DS) particles for the first, second, and third characterization studies

	First characterization				Second characterization				Third characterization			
	>2.5 μm		<2.5 μm		>2.5 μm		<2.5 μm		>2.5 μm		<2.5 μm	
Particle class	%US	%DS	%US	%DS	%US	%DS	%US	%DS	%US	%DS	%US	%DS
Uncertainty	±36	±5	±5	±3	±49	±11	±4	±3	±51	±13	±5	±3
EC-No Neg.	0	0	36	32	3	1	55	47	3	1	73	62
Long EC	0	0	2	2	0	0	2	3	0	0	2	2
Ca dust	18	17	0	1	30	14	1	2	0	12	1	1
K-sulfate-OC	0	4	21	19	15	5	8	9	3	3	4	5
EC-K-sulfate	0	0	17	18	3	1	12	12	3	1	6	8
Dust	25	25	2	4	8	23	2	6	24	27	2	5
K-phosphate	50	45	13	14	37	39	13	12	56	34	11	12
Sea salt	7	7	0	1	5	16	1	3	12	20	1	4
OC	0	0	8	9	0	1	7	6	0	0	1	2
No ID	0	1	0	1	0	2	0	1	0	0	0	0

The uncertainty refers to the entire column since it is normalized.

were performed. A general comparison was made of the overall particle composition upstream and downstream of the concentrator during periods where we switched the sampling lines between the two locations. No overall increase in ion intensities was observed for particles downstream of the concentrator relative to upstream values. This was determined by comparing the particle types obtained in two separate ART-2a analyses performed on the upstream and downstream particles. No new particle types were observed for particles detected in the outlet flow that were not detected in the inlet stream. We also examined the digital mass spectra (Liu et al. 2003) of the ten major particle types to determine if there was a fractional (or area) increase or decrease in the most likely semivolatile species (i.e., ammonium, amines, nitrate, and OC species). Again, no change was observed, further supporting the fact that no material was added or lost from the particles during the concentration process.

Table 2 also shows that the majority of the particles in the fine-mode are classified as either EC or OC, whereas coarse-mode particles are mostly dust and inorganic potassium types as observed during the exposure studies. The size–composition relationship reflects the sources and mechanism of formation of the individual particles. For example, EC and OC are expected to be in the fine-mode since they are generated by combustion processes, and the coarse-mode particles consist mainly of dust generated by mechanical or abrasion processes.

The percentages of particle classes during the 2 h human exposure studies were also examined and are shown in the pie charts of Figure 10. During the first exposure, when no condensation occurred ($T_s > T_d$), there were fewer organics in both the coarse and fine modes than there were during the second exposure, when condensation was occurring ($T_s < T_d$). Large amounts of biogenic organic compounds such as the reaction products of terpenes with ozone have been identified in the Chapel Hill region (Edney et al. 2003; Hagerman et al. 1997), and they are known to be hygroscopic due to their polar nature. Because of their hygroscopicity, these particles will attract liquid water and grow larger when conditions of saturation are reached. It is also possible that particle types other than OC will become coated with water and take up these hydrophilic compounds. Correspondingly, organics ($m/z = 12$, 27, and 43) were found to contribute to the coarse mode during the second exposure, study when condensation was occurring as shown by the pie charts of Figure 10. From the pie charts, it is evident that during the first exposure there were fewer organics present than in the second exposure, when the temperature and humidity were higher. Since the wind direction remained relatively constant during the week when the two exposures were performed, the change in the amount of organics in the coarse mode was likely due to other conditions such as temperature and RH.

Temporal Evolution of Particle Classes during Exposure Studies

The ability of the ATOFMS to track particle classes in very short time periods can provide important composition information for relatively short exposure studies. Figure 10a shows the temporal profile for concentrated particles during the first 2 h exposure study conducted on 8/25/03. The raw counts for each particle class are plotted with a temporal resolution of 10 min. The most noticeable temporal trend during the first exposure was the decrease of the K-Phosphate class and the increase of the EC class as time progressed from ~10:50 to the end of the exposure. Figure 10b shows the temporal evolution of the same classes for the second 2 h exposure study conducted on 8/27/03. During this study, the sampling location of the ATOFMS was switched between the concentrated and nonconcentrated aerosol streams. The concentrated aerosol stream was sampled for two 45 min time periods, and the nonconcentrated stream was sampled for two 15-min time periods. These different time periods are separated by the vertical lines in Figure 10b. When the sampling location was switched from concentrated to nonconcentrated, there was a sharp increase in the EC and OC particle types, while a corresponding decrease occurred in the inorganic particle classes such as dust. This is expected, given that the EC and OC classes occur in the fine- mode and inorganic particle types predominantly occur in the coarse-mode. The less-abundant classes shown in Figures 10a and 10b do not show as much temporal variation, most likely due to their low frequency of detection during the short 10-min time period used for this analysis. A comparison of the results from these two exposures shows how coarse-particle composition (and their associated sources) can vary over short time periods.

Additional measurements run alongside the ATOFMS would greatly compliment the semiquantitative data from the ATOFMS. Past measurements using a micro orfice uniform deposit impactor (MOUDI) have been used to produce quantitative results from the ATOFMS data (Bhave et al. 2002). In this previous study, the time resolution was restrained to 4 h intervals to collect enough mass with the MOUDI, but with the elevated mass exiting the concentrator the time resolution could likely be increased in a similar study. Having this additional information would also be important from a toxicological perspective, allowing the comparison of species concentrations and particle size with human response.

Comparison of the particles sampled during these two exposure studies demonstrates how even for coarse particles, the composition of the particles can vary significantly over time. In order to develop a better understanding of the health effects of particles, it is important to be able to go beyond studies that differentiate coarse versus fine particles, because the dominant composition (i.e., inorganic versus organic) or source of particles in a given size range can change, making interpretation of the health effects results difficult (Brunekreef 2002). Having the ability to track the particle mixing state will ultimately allow for linking the observed particle compositions to specific sources upon comparison with source fingerprints obtained in single-particle source characterization studies. This may make it possible to reach the ultimate goal of linking health effects with specific PM sources.

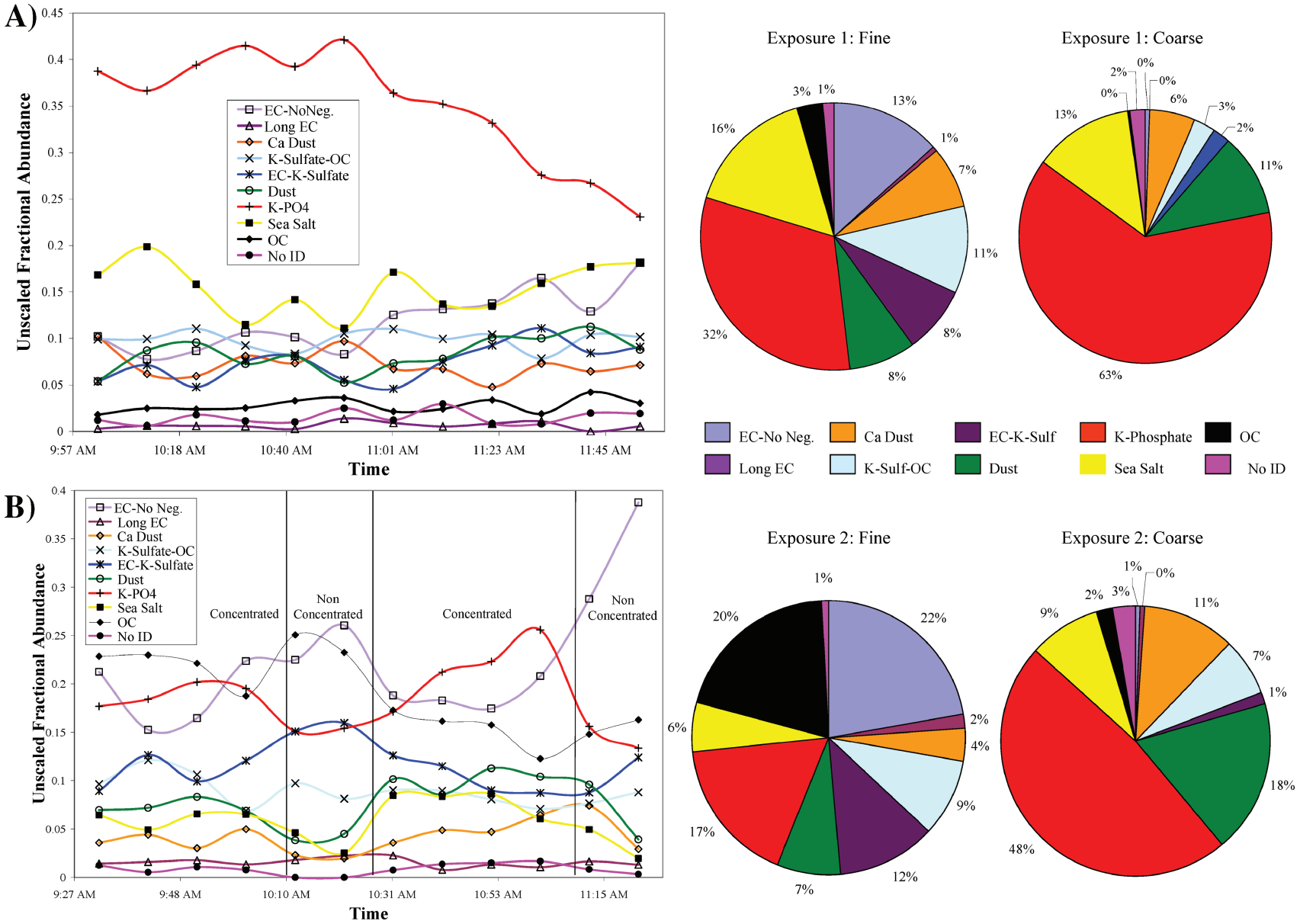

Figure 10. Temporal profiles for the major particle classes during (A) the first 2 h exposure study on 8/25/03 and (B) the second 2 h exposure study on 8/27/03. The sampling locations were changed from concentrated to nonconcentrated as illustrated by the vertical lines. The pie charts show fractional abundance during both the exposure studies.

CONCLUSIONS

The coarse particle concentrator used for human exposure studies did not cause significant chemical changes of particles between the inlet and the outlet of the concentrator itself. Since hygroscopic species are abundant in this region of the country, the dynamics involving these particles should be kept in mind while interpreting results from human exposure studies. Changes in ambient temperature and RH probably cause a variation in the amount of organic and semivolatile species found in coarse-mode particles from day to day. This was seen in this study as an increase in organics during the exposure when the dew point temperature of the aerosol stream exceeded the sampling temperature. One possible way to avoid changing the chemical composition artificially would be to match the temperature of the concentrator and sampling lines to ambient temperatures somehow, as well as match the RH of the dilution air to the ambient RH.

The size distributions for the inlet and outlet of the concentrator were characterized along with their associated concentration factors with the use of the APS instruments. The concentration factor for coarse-mode ambient particles was found to be around 50 or 60—a value within good agreement with the laboratory characterization of the concentrator. Concentration factors for fine-mode particles which showed an increase from 2–46 for the 0.54–2.5 μm size range.

This study additionally showed the variability of coarse particle composition during short 2 h exposures, detecting chemical changes in concentrated ambient aerosol at a time resolution of 10 min. Relating the chemical classes to sources and a comparison of the exposure data with bulk measurements is work currently in progress and will be presented in the near future.

REFERENCES

Allen, J. O., Fergenson, D. P., Gard, E. E., Hughes, L. S., Morrical, B. D., Kleeman, M. J., Gross, D. S., Galli, M. E., Prather, K. A., and Cass, G. R. (2000). Particle Detection Efficiencies of Aerosol Time of Flight Mass Spectrometers under Ambient Sampling Conditions, *Environ. Sci. Technol.* 34:211–217.

Angelino, S., Suess, D. T., and Prather, K. A. (2001). Formation of Aerosol Particles from Reactions of Secondary and Tertiary Alkylamines: Characterization by Aerosol Time-of-Flight Mass Spectrometry, *Environ. Sci. Technol.* 35:3130–3138.

Bhave, P. V., Allen, J. O., Morrical, B. D., Fergenson, D. P., Cass, G. R., and Prather, K. A. (2002). A Field-Based Approach for Determining ATOFMS Instrument Sensitivities to Ammonium and Nitrate, *Environ. Sci. Technol.* 36:4868–4879.

Brunekreef, B., and Holgate, S. T. (2002). Air Pollution and Health, *Lancet* 360:1233–1242.

Cornell, S. E., Jickells, T. D., Cape, J. N., Rowland, A. P., and Duce, R. A. (2003). Organic Nitrogen Deposition on Land and Coastal Environments: A Review of Methods and Data, *Atmos. Environ.* 37:2173–2191.

Demokritou, P., Gupta, T., Ferguson, S., and Koutrakis, P. (2003). Development of a High-Volume Concentrated Ambient Particles System (Caps) for Human and Animal Inhalation Toxicological Studies, *Inhal. Toxicol.* 15: 111–129.

Dockery, D. W., and Pope, C. A. (1994). Acute Respiratory Effects of Particulate Air-Pollution, *Ann. Rev. Pub. Health* 15:107–132.

Dockery, D. W., Pope, C. A., Xu, X. P., Spengler, J. D., Ware, J. H., Fay, M. E., Ferris, B. G., and Speizer, F. E. (1993). An Association between Air-Pollution and Mortality in 6 United-States Cities, *N. Engl. J. Med.* 329:1753–1759.

Dockery, D. W., Schwartz, J., and Spengler, J. D. (1992). Air-Pollution and Daily Mortality—Associations with Particulates and Acid Aerosols, *Environ. Res.* 59:362–373.

Eatough, D. J., Long, R. W., Modey, W. K., and Eatough, N. L. (2003). Semi-Volatile Secondary Organic Aerosol in Urban Atmospheres: Meeting a Measurement Challenge, *Atmos. Environ.* 37:1277–1292.

Edney, E. O., Kleindienst, T. E., Conver, T. S., McIver, C. D., Corse, E. W., and Weathers, W. S. (2003). Polar Organic Oxygenates in $PM_{2.5}$ at a Southeastern Site in the United States, *Atmos. Environ.* 37:3947–3965.

Finlayson-Pitts, B. J., and Pitts, J. N. (2000). Chemistry of the Upper and Lower Atmosphere: Theory, Experiments, and Applications. Academic Press, San Diego, CA.

Gamble, J. F. (1998). $PM_{2.5}$ and Mortality in Long-Term Prospective Cohort Studies: Cause-Effect or Statistical Associations? *Environ. Health Persp.* 106:535–549.

Gard, E., Mayer, J. E., Morrical, B. D., Dienes, T., Fergenson, D. P., and Prather, K. A. (1997). Real-Time Analysis of Individual Atmospheric Aerosol Particles: Design and Performance of a Portable ATOFMS, *Anal. Chem.* 69:4083–4091.

Gavett, S. H., and Koren, H. S. (2001). The Role of Particulate Matter in Exacerbation of Atopic Asthma, *Int. Arch. Allergy Immunol.* 124:109–112.

Guazzotti, S. A., Suess, D. T., Coffee, K. R., Quinn, P. K., Bates, T. S., Wisthaler, A., Hansel, A., Ball, W. P., Dickerson, R. R., Neususs, C., Crutzen, P. J., and Prather, K. A. (2003). Characterization of Carbonaceous Aerosols Outflow from India and Arabia: Biomass/Biofuel Burning and Fossil Fuel Combustion, *J. Geophys. Res.-Atmos*. 108:4485–4499.

Guazzotti, S. A., Whiteaker, J. R., Suess, D., Coffee, K. R., and Prather, K. A. (2001). Real-Time Measurements of the Chemical Composition of Size-Resolved Particles during a Santa Ana Wind Episode, California, USA, *Atmos. Environ*. 35:3229–3240.

Hagerman, L. M., Aneja, V. P., and Lonneman, W. A. (1997). Characterization of Non-Methane Hydrocarbons in the Rural Southeast United States, *Atmos. Environ.* 31:4017–4038.

Hinds, W. C. (1999). Aerosol Technology, John Wiley & Sons, Inc., New York.

Hughes, L. S., Allen, J. O., Bhave, P., Kleeman, M. J., Cass, G. R., Liu, D. Y., Fergenson, D. F., Morrical, B. D., and Prather, K. A. (2000). Evolution of Atmospheric Particles Along Trajectories Crossing the Los Angeles Basin, *Environ. Sci. Technol*. 34:3058–3068.

Leikauf, G. D. (2002). Hazardous Air Pollutants and Asthma, *Environ. Health Pers.* 110:505–526.

Lippmann, M. (1989). Background on Health-Effects of Acid Aerosols, *Environ. Health Pers.* 79:3–6.

Liu, D. Y., Wenzel, R. J., and Prather, K. A. (2003). Aerosol Time-of-Flight Mass Spectrometry During the Atlanta Supersite Experiment: 1. Measurements, *J. Geophys. Res.—Atmos*. 108:8426–8442.

Monn, C., and Becker, S. (1999). Cytotoxicity and Induction of Proinflammatory Cytokines from Human Monocytes Exposed to Fine ($PM_{2.5}$) and Coarse Particles ($PM_{10-2.5}$) in Outdoor and Indoor Air, *Toxicol. Appl. Pharm.* 155:245–252.

Neubauer, K. R., Johnston, M. V., and Wexler, A. S. (1997). On-Line Analysis of Aqueous Aerosols by Laser Desorption Ionization, *Int. J. Mass Spectrom. Ion Proc.* 163:29–37.

Noble, C. A., and Prather, K. A. (1997). Real-time Single Particle Monitoring of a Relative Increase in Marine Aerosol Concentration During Winter Rainstorms, *Geophys. Res. Lett*. 24:2753–2756.

Peters, A., Dockery, D. W., Heinrich, J., and Wichmann, H. E. (1997). Short-Term Effects of Particulate Air Pollution on Respiratory Morbidity in Asthmatic Children, *Eur. Resp. J.* 10:872–879.

Rice, T. J., Buol, S. W., and Weed, S. B. (1985). Soil Saprolite Profiles Derived from Mafic Rocks in the North Carolina Piedmont: I. Chemical, Morphological and Mineralogical Characteristics and Transformations, *Soil. Sci. Soc. Am. J.* 49:171–178.

Robarge, W. P., Walker, J. T., McCulloch, R. B., and Murray, G. (2002). Atmospheric Concentrations of Ammonia and Ammonium at an Agricultural Site in the Southeast United States, *Atmos. Environ.* 36:1661–1674.

Seagrave, J., Mauderly, J. L., and Seilkop, S. K. (2003). In Vitro Relative Toxicity Screening of Combined Particulate and Semivolatile Organic Fractions of Gasoline and Diesel Engine Emissions, *J. Toxicol. Environ. Health A* 66:1113–1132.

Silva, P. J., Carlin, R. A., and Prather, K. A. (2000). Single Particle Analysis of Suspended Soil Dust from Southern California, *Atmos. Environ*. 34:1811–1820.

Silva, P. J., and Prather, K. A. (2000). Chapter 6: Characterization of Individual Particles Emitted from the Charbroiling of Meat. PhD Thesis, Department of Chemistry, University of California Riverside, Riverside, 189–208.

Song, X. H., Hopke, P. K., Fergenson, D. P., and Prather, K. A. (1999). Classification of Single Particles Analyzed by ATOFMS Using an Artificial Neural Network, ART-2a, *Anal. Chem*. 71:860–865.

Tobias, H. J. K., Peter, M., Docherty, K. S., and Ziemann, P. J. (2000). Real-Time Chemical Analysis of Organic Aerosols Using a Thermal Desorption Particle Beam Mass Spectrometer, *Aerosol Sci. Technol.* 33:170–190.

Walker, J. T., Aneja, V. P., and Dickey, D. A. (2000). Atmospheric Transport and Wet Deposition of Ammonium in North Carolina, *Atmos. Environ.* 34:3407–3418.

Wenzel, R. J., and Prather, K. A. (2004). Improvements in Ion Signal Reproducibility Obtained Using a Homogeneous Laser Beam for On-Line Laser Desorption/Ionization of Single Particles, *Rapid Comm. Mass Spectrom.* 18:1525–1533.